J|A|C|S
ARTICLES
Published on Web 04/07/2007

Determining the Orientation of Uniaxially Rotating Membrane Proteins Using Unoriented Samples: A ^{2}H, ^{13}C, and ^{15}N Solid-State NMR Investigation of the Dynamics and Orientation of a Transmembrane Helical Bundle

Sarah D. Cady,[†] Catherine Goodman,[‡] Chad D. Tatko,[‡] William F. DeGrado,[‡] and Mei Hong*,[†]

Contribution from the Department of Chemistry, Iowa State University, Ames, Iowa 50011, and Department of Biochemistry and Biophysics, University of Pennsylvania, School of Medicine, Philadelphia, Pennsylvania 19104-6059

Received January 15, 2007; E-mail: mhong@iastate.edu

Abstract: Membrane protein orientation has traditionally been determined by NMR using mechanically or magnetically aligned samples. Here we show a new NMR approach that abolishes the need for preparing macroscopically aligned membranes. When the protein undergoes fast uniaxial rotation around the bilayer normal, the 0°-frequency of the motionally averaged powder spectrum is identical to the frequency of the aligned protein whose alignment axis is along the magnetic field. Thus, one can use unoriented membranes to determine the orientation of the protein relative to the bilayer normal. We demonstrate this approach on the M2 transmembrane peptide (M2TMP) of influenza A virus, which is known to assemble into a proton-conducting tetrameric helical bundle. The fast uniaxial rotational diffusion of the M2TMP helical bundle around the membrane normal is characterized via ^{2}H quadrupolar couplings, C−H and N−H dipolar couplings, ^{13}C chemical shift anisotropies, and ^{1}H $T_{1\rho}$ relaxation times. We then show that ^{15}N chemical shift anisotropy and N−H dipolar coupling measured on these powder samples can be analyzed to yield precise tilt angles and rotation angles of the helices. The data show that the tilt angle of the M2TMP helices depends on the membrane thickness to reduce the hydrophobic mismatch. Moreover, the orientation of a longer M2 peptide containing both the transmembrane domain and cytoplasmic residues is similar to the orientation of the transmembrane domain alone, suggesting that the transmembrane domain regulates the orientation of this protein and that structural information obtained from M2TMP may be extrapolated to the longer peptide. This powder-NMR approach for orientation determination is generally applicable and can be extended to larger membrane proteins.

Introduction

Orientation determination of membrane proteins by solid-state NMR traditionally requires mechanically or magnetically aligned proteins.[1,2] A uniaxially aligned protein produces resolved spectra where the anisotropic frequency (chemical shift or dipolar coupling) reports the orientation of the molecule-fixed spin interaction tensor, from which the orientation of the protein can be obtained. However, this approach is constrained by the degree of alignment. Poor alignment can occur for many reasons: (i) the size of the protein may be too large; (ii) the protein−lipid molar ratio may be too high, which is important for achieving sufficient sensitivity but deleterious for alignment; (iii) the protein may be inherently membrane disruptive by causing curvature and nonlamellar phases.[3,4] Often only a narrow set of lipids is conducive to alignment for a specific protein, thus the dependence of orientation on environmental parameters such as membrane thickness and membrane composition is difficult to study. These factors severely restrict the determination of membrane protein orientation.

It is thus desirable to develop alternative approaches for determining membrane protein orientation that do not require macroscopic alignment but instead use straightforward unoriented liposomes. We demonstrate here that this is possible as long as the membrane protein undergoes fast uniaxial rotational diffusion around the bilayer normal compared to the time scale of the NMR spin interactions. Under this condition, the protein orientation can be extracted with high precision using unoriented membranes and magic-angle spinning (MAS) or static experiments. The elimination of macroscopic alignment also increases the sample amount in the radiofrequency (rf) coil by removing the alignment media, giving higher sensitivity.

The M2 protein of the influenza A virus is a well-studied proton channel that initiates the release of the viral ribonuclear protein complex into the host cell, which is necessary for viral

[†] Iowa State University.
[‡] University of Pennsylvania.

(1) Opella, S. J.; Marassi, F. M. *Chem. Rev.* **2004**, *104*, 3587−3606.
(2) Hong, M. *Structure* **2006**, *14*, 1731−1740.
(3) Buffy, J. J.; McCormick, M. J.; Wi, S.; Waring, A.; Lehrer, R. I.; Hong, M. *Biochemistry* **2004**, *43*, 9800−9812.
(4) Hallock, K. J.; Lee, D. K.; Ramamoorthy, A. *Biophys. J.* **2003**, *84* (5), 3052−3060.

replication.[5,6] The transmembrane domain of the M2 protein, M2TMP (residues 22−46), has been extensively studied by a number of biophysical techniques, including electrophysiological measurements,[7,8] analytical ultracentrifugation,[9,10] solid-state NMR,[11,12] neutron diffraction,[13] and molecular dynamics simulation.[14−17] The results indicate that M2TMP has the essential characteristics of the intact protein: it forms tetrameric helical bundles with proton-conducting abilities in the lipid membrane.[18] Cross and co-workers used glass-plate aligned membranes and 2D ^{15}N correlation experiments to show that the helices in this tetrameric bundle are tilted by 38° ± 3°[11] from the bilayer normal in DMPC bilayers. The availability of this information makes M2TMP an excellent model system to test the principle of orientation determination using powder samples. Moreover, the orientation of M2TMP has been measured in detail only in DMPC (14:0) bilayers. A more limited set of NMR data on M2TMP bound to DOPC bilayers, which have longer acyl chains (18:1) than DMPC (14:0), found an orientation similar to that in DMPC bilayers.[19] This was interpreted to suggest that M2TMP orientation is an inherent property of the protein and is independent of the membrane thickness. However, a more recent EPR study of M2TMP bound to DLPC, DMPC, POPC, and DOPC bilayers suggested that the peptide orientation does change with the membrane thickness.[20] Thus, further experiments are of interest to resolve this discrepancy.

Another issue investigated in the current paper is the role of a C-terminal helix in M2, which occurs just beyond the transmembrane helix. Previously, limited proteolysis of full-length M2 protein in micelles and CD spectroscopy were used to identify a cytoplasmic amphiphilic helix that follows the transmembrane helix in the sequence of M2.[21] The C-terminal helix increases the stability of the tetramer (relative to a peptide spanning only the TM helix), and this cytoplasmic helix was also essential to obtain full proton channel activity when deletion mutants were expressed in oocytes.[7] The role of this C-terminal segment in stabilizing the channel is currently not known. Originally, it was suggested that the cytoplasmic helix might have one of two orientations: in one model it formed an extension of the transmembrane helix, possibly explaining the increased stability of the tetramer. In a second model, the helix was proposed to lie parallel to the membrane surface, radiating out from the transmembrane helix bundle in a rosette-like structure with a radius of 35−40 Å.[21] Subsequent solid-state NMR studies of the full-length M2 protein[22] were more consistent with the rosette model, although there were also features in these experiments that were difficult to understand. Hydrogen−deuterium exchange data indicated that the amide NH groups of all residues in the transmembrane helix exchanged with solvent very rapidly, irrespective of whether they faced the phospholipid acyl chains or the transmembrane pore. By contrast, in the cytoplasmic helix the putative lipid-facing amides were found to exchange very slowly with the bulk water.[22] However, because the studies were not conducted with site-specifically labeled proteins, there remained some ambiguity in the conclusions. Thus, in this paper, we include initial data on a 42-residue peptide including both the transmembrane and the cytoplasmic helix.

In this work, we first examine the rotational dynamics of the M2TMP helical bundle under different sample preparation conditions and in lipid bilayers of different thicknesses. Multiple NMR spin interactions, including ^{2}H quadrupolar couplings, ^{13}C chemical shift anisotropy (CSA), C−H dipolar couplings, and ^{1}H rotating-frame relaxation time ($T_{1\rho}$), are used to examine the amplitude and rate of M2TMP rotational diffusion. We then measure the ^{15}N−^{1}H dipolar couplings and ^{15}N CSAs of site-specifically labeled M2TMP in unoriented membranes under MAS or static conditions. These anisotropic couplings are summarized in the same 2D correlation patterns—"PISA" wheels—as those obtained from oriented membrane samples. These powder PISA wheel spectra show that the orientation of M2TMP does depend on the lipid bilayer thickness: it decreases from 35° ± 3° in DLPC bilayers to 26° ± 3° in POPC bilayers. Finally, we show that the longer segment of the M2 protein encompassing both the transmembrane domain and cytoplasmic residues has the same orientation in DLPC bilayers as M2TMP, suggesting that the transmembrane domain regulates the orientation of the protein.

Materials and Methods

Peptides and Lipids. 1-Palmitoyl-2-oleoyl-*sn*-glycero-3-phosphocholine (POPC), 1,2-dimyristoyl-*sn*-glycero-3-phosphocholine (DMPC), and 1,2-dilauroyl-*sn*-glycero-3-phosphocholine (DLPC) were obtained from Avanti Polar Lipids (Alabaster, AL). ^{13}C-, ^{2}H-, and ^{15}N-labeled Leu and Val (Sigma) were FMOC-protected in house using standard methods.[23] Other FMOC-protected amino acids were purchased from Sigma (Miamisburg, OH) and Cambridge Isotope Laboratories (Andover, MA).

The transmembrane domain (residues 22−46) of the M2 protein of the A/Udorn/307/72 (H3N2) influenza A virus (SSDPLVVAASIIGILHLILWILDRL)[24] was synthesized and purified by Primm Biotech (Cambridge, MA). These samples contain various site-specific ^{2}H, ^{13}C, and ^{15}N labels. One sample contains an L38F mutation to allow a 4-^{19}F label at the phenylene ring. This L38F variant is found in the Weybridge (FPVW27) strain of the influenza A virus[24] and has similar biological activity as the Udorn strain.[25]

(5) Lamb, R. A.; Holsinger, K. J.; Pinto, L. H. *Cellular Receptors of Animal Viruses*; Wemmer, E., Ed.; Cold Spring Harbor Lab Press: Plainview, NY, 1994; pp 303−321.
(6) Pinto, L. H.; Lamb, R. A. *J. Biol. Chem.* **2006**, *281* (14), 8997−9000.
(7) Pinto, L. H.; Holsinger, L. J.; Lamb, R. A. *Cell* **1992**, *69* (3), 517−528.
(8) Tang, Y.; Zaitseva, F.; Lamb, R. A.; Pinto, L. H. *J. Biol. Chem.* **2002**, *277* (42), 39880−39886.
(9) DeGrado, W. F.; Gratkowski, H.; Lear, J. D. *Protein Sci.* **2003**, *12*, 647−665.
(10) Howard, K. P.; Lear, J. D.; DeGrado, W. F. *Proc. Natl. Acad. Sci. U.S.A.* **2002**, *99* (13), 8568−8572.
(11) Wang, J.; Kim, S.; Kovacs, F.; Cross, T. A. *Protein Sci.* **2001**, *10* (11), 2241−2250.
(12) Nishimura, K.; Kim, S.; Zhang, L.; Cross, T. A. *Biochemistry* **2002**, *41* (44), 13170−13177.
(13) Duff, K. C.; Gilchrist, P. J.; Saxena, A. M.; Bradshaw, J. P. *Virology* **1994**, *202* (1), 287−293.
(14) Wu, Y.; Voth, G. A. *Biophys. J.* **2005**, *89*, 2402−2411.
(15) Fischer, W. B.; Sansom, M. S. *Biochim. Biophys. Acta.* **2002**, *1561*, 27−45.
(16) Zhong, Q.; Husslein, T.; Moore, P. B.; Newns, D. M.; Pattnaik, P.; Klein, M. L. *FEBS Lett.* **1998**, *434*, 265−271.
(17) Zhong, Q.; Newns, D. M.; Pattnaik, P.; Lear, J. D.; Klein, M. L. *FEBS Lett.* **2000**, *473*, 195−198.
(18) Luo, W.; Hong, M. *J. Am. Chem. Soc.* **2006**, *128*, 7242−7451.
(19) Kovacs, F. A.; Cross, T. A. *Biophys. J.* **1997**, *73*, 2511−2517.
(20) Duong-Ly, K. C.; Nanda, V.; Degrado, W. F.; Howard, K. P. *Protein Sci.* **2005**, *14*, 856−861.
(21) Kochendoerfer, G. G.; Salom, D.; Lear, J. D.; Wilk-Orescan, R.; Kent, S. B.; DeGrado, W. F. *Biochemistry* **1999**, *38*, 11905−11913.
(22) Tian, C.; Tobler, K.; Lamb, R. A.; Pinto, L. H.; Cross, T. A. *Biochemistry* **2002**, *41*, 11294−11300.
(23) Carpino, L. A.; Han, G. Y. *J. Org. Chem.* **1972**, *37* (22), 3404−3409.
(24) Ito, T.; Gorman, O. T.; Kawaoka, Y.; Bean, W. J.; Webster, R. G. *J. Virol.* **1991**, *65* (10), 5491−5498.
(25) Wang, C.; Takeuchi, K.; Pinto, L. H.; Lamb, R. A. *J. Virol.* **1993**, *67* (9), 5585−5594.

Membrane Sample Preparation. Peptide-containing membrane samples were prepared either by an aqueous-phase mixing method or by an organic-phase mixing method. The aqueous samples were prepared by mixing the peptide with pH 7.5 lipid vesicle solutions at a peptide/lipid molar ratio (P/L) of 1:15. The lipid solution was vortexed, freeze/thawed 6−8 times to create uniform vesicles of <200 nm diameter,[26] and then added to the appropriate amount of M2TMP. The solution was incubated at 30 °C for 2 days, after which it was ultracentrifuged at 150000*g* for 3 h above the lipid main phase transition (T_m) temperature. The resulting pellet typically contained ∼50% water by mass. UV−vis absorption and a photometric assay of the supernatant[27,28] showed that ∼98% of the peptide is bound to the pellet. The organic-phase mixed samples used P/L = 1:20 and were prepared by codissolving M2TMP with lipids in trifluoroethanol, drying the mixture with nitrogen gas, redissolving it in cyclohexane, lyophilizing, and then rehydrating to 50% water by mass using a phosphate buffer (pH 8.1). We refer to these two types of samples as "aqueous samples" and "organic samples", even though the final products are both well-hydrated proteoliposomes.

Importantly, we have confirmed by independent ^{19}F spin diffusion experiments that the oligomeric state of M2TMP is indeed tetramer at the peptide concentrations used here, whether the sample is prepared by aqueous-phase mixing or organic-phase mixing.[18,29] This is manifested as an equilibrium value of ∼0.25 at long spin diffusion mixing times. Thus, the mobility and orientation observed in this work are those of the tetrameric M2 peptide.

Solid-State NMR Spectroscopy. NMR experiments were carried out on a Bruker AVANCE-600 (14.1 T) spectrometer and a DSX-400 (9.4 T) spectrometer (Karlsruhe, Germany). The ^{2}H experiments were carried out using a quadrupolar echo pulse sequence with a ^{2}H 90° pulse length of 5 μs. Static ^{15}N chemical shift spectra were measured using a Hahn-echo sequence. ^{13}C−^{1}H and ^{15}N−^{1}H dipolar couplings were measured using the 2D DIPSHIFT experiment[30] at 2.4−3.5 kHz MAS with MREV-8 for ^{1}H homonuclear decoupling. Pulse lengths of 3.5−5.2 μs were used in the MREV-8 pulse train, the longer values due to the rf power loss on some of the hydrated membrane samples. Tests on the model compound ^{15}N-acetyl-valine indicate that the measured dipolar coupling is unaffected by the varying MREV-8 field strengths within the range used. The N−H DIPSHIFT experiments were performed with dipolar doubling[31,32] to increase the precision of the measured couplings. The ^{13}C chemical shift anisotropy (CSA) was measured using the 2D SUPER experiment[33] under 2.5 kHz MAS. The corresponding ^{13}C field strength was 30.3 kHz. ^{1}H $T_{1\rho}$ was measured using a spin-lock field strength of 62.5 kHz.

The ^{2}H and ^{13}C 1D spectra were recorded between 243 and 313 K. All ^{15}N chemical shift and N−H dipolar coupling experiments were carried out at 313 K where the peptide is mobile to determine the helix orientation.

Results and Discussion

Equivalence of Aligned and Powder Samples for Uniaxially Mobile Molecules. For a membrane protein undergoing fast uniaxial rotational diffusion around the bilayer normal, the 0°-frequency, $\bar{\delta}_{||}$, of the motionally average powder spectrum is identical to the frequency when the protein is uniformly aligned, with the alignment axis parallel to the magnetic field (0°-aligned sample):[34]

$$\bar{\delta}_{||} = \omega_{0°aligned} = \frac{1}{2}\delta(3\cos^2\theta - 1 - \eta\sin^2\theta\cos 2\phi) + \omega_{iso} \quad (1)$$

Here $\delta = \delta_{zz} - \delta_{iso}$ and $\eta = (\delta_{yy} - \delta_{xx})/\delta$ are the anisotropy and asymmetry parameters, respectively, of the rigid-limit interaction tensor. The angles (θ, ϕ) are the polar coordinates of the magnetic field B_0 in the principal axis system of the spin interaction tensor. Equation 1 can be derived, as we showed recently,[34] by considering the frequency of an aligned sample without motion, then the frequency of an aligned sample undergoing uniaxial rotation around the alignment axis of bilayer normal, then the motionally averaged anisotropy parameter of the same aligned and mobile sample, and finally the powder spectrum of the mobile sample without alignment. The essential link between the frequency of a 0°-aligned sample and that of an unoriented sample is that $\bar{\delta}_{||}$ of the motionally averaged powder pattern is obtained when B_0 is along the motional axis, the bilayer normal. This is identical to the geometry of a 0°-aligned sample, when B_0 coincides with the alignment axis, also the bilayer normal.

Once $\bar{\delta}_{||}$ is known, the motionally averaged anisotropy parameter, $\bar{\delta}$, and the frequency of the powder pattern maximum, $\bar{\delta}_{\perp}$, are also known, since these are related by

$$\bar{\delta}_{\perp} - \omega_{iso} = -\frac{1}{2}(\omega_{0°aligned} - \omega_{iso}) = -\frac{1}{2}(\bar{\delta}_{||} - \omega_{iso}) = -\frac{1}{2}\bar{\delta} \quad (2)$$

Thus, one can extract the orientation information by measuring the high-sensitivity $\bar{\delta}_{\perp}$ (90°) edge, rather than the low-intensity $\bar{\delta}_{||}$ edge, of the uniaxially averaged spectrum.

Predicted Rates of Rotational Diffusion of Membrane Proteins. The prerequisite for this powder-sample orientation determination approach is that the membrane protein must undergo uniaxial rotational diffusion at a rate larger than the NMR spin interaction. The rotational diffusion rate of proteins in two-dimensional membranes is given by the Saffman−Delbrück equation:[35]

$$D_r = \frac{kT}{4\pi\eta r^2 h} \quad (3)$$

where the diffusion coefficient D_r is directly proportional to the temperature T and inversely proportional to the membrane viscosity η, the square of the radius (r) of the diffusing cylinder, and the height (h) of the cylinder.

Equation 3 allows us to estimate the diffusion rates of membrane proteins of varying sizes. Figure 1 plots the calculated rotational diffusion rates D_r as a function of r at $T = 298$ K, with $h = 19.5$ Å for DLPC bilayers and 27 Å for POPC bilayers, and assuming a membrane viscosity of 10 poise,[35] A single TM α-helix, which has a radius of ∼5 Å, gives a D_r of ∼6.7×10^5

(26) Traikia, M.; Warschawski, D. E.; Recouvreur, M.; Cartaud, J.; Devaux, P. F. *Eur. Biophys. J.* **2000**, *29* (3), 184−195.
(27) Pace, C. N.; Vajdos, F.; Fee, L.; Grimsley, G.; Gray, T. *Protein Sci.* **1995**, *4* (11), 2411−2423.
(28) Smith, P. K.; Krohn, R. I.; Hermanson, G. T.; Mallia, A. K.; Gartner, F. H.; Provenzano, M. D.; Fujimoto, E. K.; Goeke, N. M.; Olson, B. J.; Klenk, D. C. *Anal. Biochem.* **1985**, *150*, 76−85.
(29) Luo, W.; Mani, R.; Hong, M. *Biochemistry* **2007**. Manuscript submitted.
(30) Munowitz, M. G.; Griffin, R. G.; Bodenhausen, G.; Huang, T. H. *J. Am. Chem. Soc.* **1981**, *103*, 2529−2533.
(31) Hong, M.; Gross, J. D.; Rienstra, C. M.; Griffin, R. G.; Kumashiro, K. K.; Schmidt-Rohr, K. *J. Magn. Reson.* **1997**, *129*, 85−92.
(32) Huster, D.; Yamaguchi, S.; Hong, M. *J. Am. Chem. Soc.* **2000**, *122*, 11320−11327.
(33) Liu, S. F.; Mao, J. D.; Schmidt-Rohr, K. *J. Magn. Reson.* **2002**, *155* (1), 15−28.
(34) Hong, M.; Doherty, T. *Chem. Phys. Lett.* **2006**, *432*, 296−300.
(35) Saffman, P. G.; Delbruck, M. *Proc. Natl. Acad. Sci. U.S.A.* **1975**, *72* (8), 3111−3113.

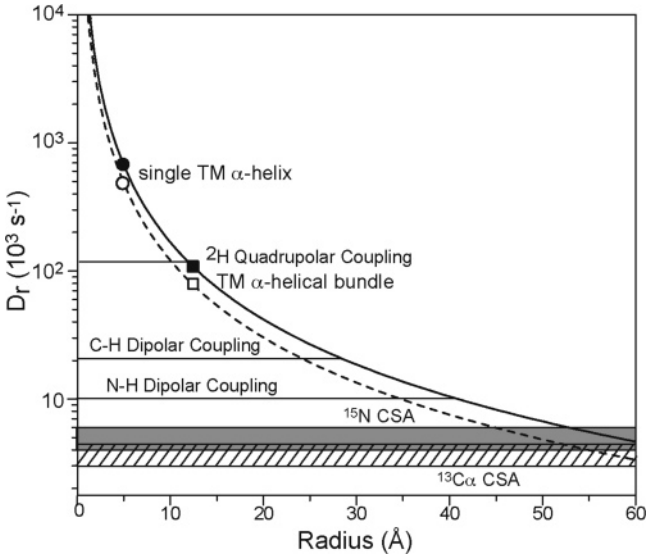

Figure 1. Calculated rotational diffusion rates of membrane proteins as a function of radius compared to various NMR spin interactions. The rotational rates of a single TM α-helix (circles) and a tetrameric α-helical bundle (squares) are indicated. For the calculated curves, a membrane viscosity of 10 poise and a temperature of 298 K are used. A diffusion cylinder with a height (*h*) of 19.5 Å (solid line) and 27 Å (dashed line) are used, corresponding to the hydrophobic thickness of DLPC and POPC bilayers, respectively. Superimposed are the ^{2}H quadrupolar coupling strength, C−H and N−H dipolar couplings, and ^{15}N and ^{13}Cα chemical shift anisotropies for magnetic field strengths of 9.4−14.1 T.

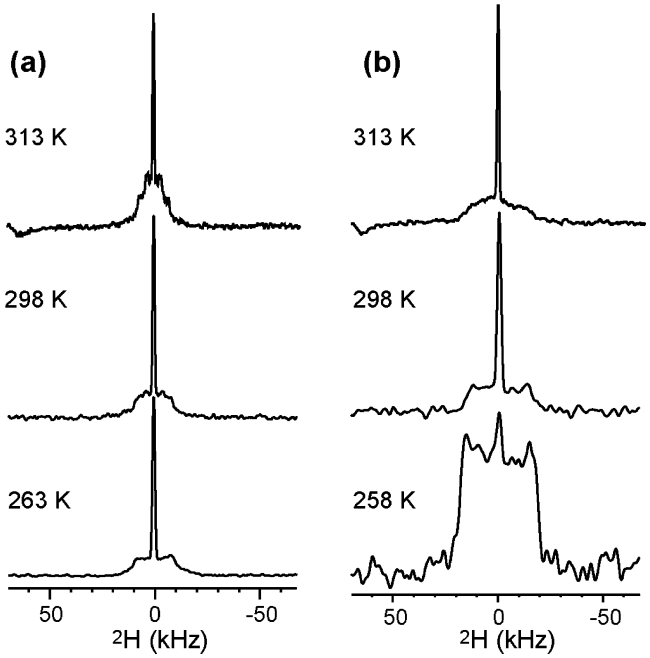

Figure 2. ^{2}H spectra of d_3-L38-M2TMP in POPC membranes prepared via (a) organic mixing and (b) aqueous mixing at various temperatures. Quadrupolar splittings of the organic sample are 13.8, 15.0, and 16.0 kHz from top to bottom (a). Quadrupolar splittings of the aqueous sample are 26.0, 26.0, and 31.0 kHz from top to bottom (b).

s^{-1} and 4.9×10^5 s^{-1} for DLPC and POPC bilayers, respectively. These rates are much larger than any spin interactions in proteins, thus a single TM helix in liquid-crystalline bilayers should give motionally narrowed spectra.

If the α-helix is surface bound instead of transmembrane, the radius of the diffusing cylinder will be on the order of the length of the helix, whereas *h* is roughly the radius of the helix. For a 25-residue α-helix, using $r = 37.5$ Å and $h = 5$ Å, we find a D_r of $\sim 4.7 \times 10^4$ s^{-1}. This is smaller than the ^{2}H quadrupolar coupling of 125 kHz. Indeed, a recent ^{2}H NMR study of an in-plane 26-residue α-helix found the peptide to be immobilized on the ^{2}H NMR time scale.[36]

A TM helical bundle has a larger *r* than a single helix and thus should have a lower rotational diffusion rate. The M2TMP tetramer is estimated to have a radius of ∼12.5 Å based on the existing structural model (PDB code: 1NYJ). The resulting D_r is $\sim 10^5$ s^{-1}, which is comparable to the ^{2}H quadrupolar interaction and much larger than any spin-$^1/_2$ interactions such as C−H dipolar couplings and ^{15}N CSA (Figure 1). Since the membrane viscosity used in the calculation is an estimated value and since *T* is an adjustable parameter, the rotational diffusion rate may exceed the ^{2}H quadrupolar interaction under experimentally accessible conditions. Certainly, the rotational diffusion of this tetrameric helical bundle is sufficiently fast to average spin-1/2 interactions.

It is important to note that the fast uniaxial rotation relevant for orientation determination is the rotation of the entire helical bundle together around the membrane normal and that the individual helices do not rotate around their own molecular axes. That the bilayer normal is the motional axis is dictated by the two-dimensional nature of the membrane, which makes intermolecular potentials symmetric around this bilayer normal. Moreover, the bundle axis is parallel to the bilayer normal, making the orientation of all helices relative to the bilayer normal identical, since only a single anisotropic NMR signal was observed for each residue.[9,11] Thus, rotation around the membrane normal is also rotation around the bundle axis.

^{2}H Spectra of M2TMP in Lipid Membranes: Conditions for Fast Uniaxial Rotation. Previous ^{15}N spectra of glass-plate aligned M2TMP with the alignment axis perpendicular to the magnetic field showed narrow peaks that indicate the presence of fast uniaxial rotation of this helical bundle.[37] However, whether this motion is fast on the time scales of larger spin interactions such as ^{2}H quadrupolar coupling is not known, and the rates and amplitudes of the motion have also not been characterized. We first measured the ^{2}H spectra of site-specifically deuterated M2TMP in various lipid membranes to provide a lower limit of the rotational diffusion rates. Figure 2 shows the ^{2}H spectra of 5,5,5-d_3-L38-M2TMP in POPC bilayers at several temperatures. In the Lα-phase of the membrane, the Leu_{38} CD_3 group experiences methyl three-site jumps, χ_1 and χ_2 torsional motion, and possible backbone motion. The methyl three-site jumps reduce the rigid-limit ^{2}H quadrupolar coupling to 40 kHz.[38] Any further coupling reduction must be a result of the two other motional mechanisms.

The ^{2}H spectra in Figure 2 show different dynamics for different sample preparation conditions. For the organic sample (a), the spectra show $\bar{\eta} = 0$ lineshapes and couplings of <15 kHz in the Lα phase (Figure 2a). For the aqueous sample, the spectra show couplings of >25 kHz and non-uniaxial lineshapes at the same temperatures. Mildly below the phase transition

(36) Aisenbrey, C.; Bechinger, B. *J. Am. Chem. Soc.* **2004**, *126* (50), 16676−16683.
(37) Song, Z.; Kovacs, F. A.; Wang, J.; Denny, J. K.; Shekar, S. C.; Quine, J. R.; Cross, T. A. *Biophys. J.* **2000**, *79*, 767−775.
(38) Palmer, A. G.; Williams, J.; McDermott, A. *J. Phys. Chem.* **1999**, *100*, 13293−13310.

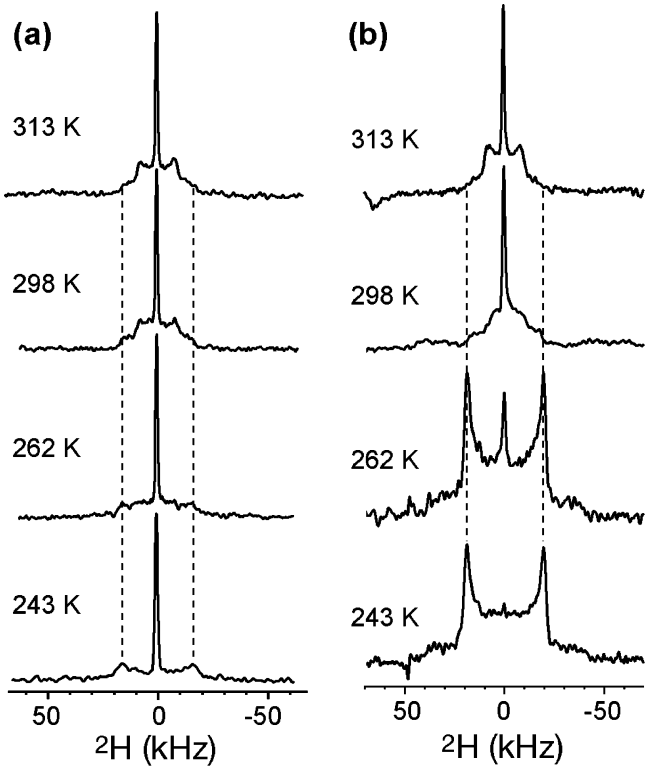

Figure 3. ^{2}H spectra of d_3-A29 L38F-M2TMP in (a) DLPC and (b) POPC membranes at various temperatures. Both samples were prepared by organic mixing. The quadrupolar splittings in (a) are 16, 16, 32, and 32 kHz from top to bottom. The quadrupolar splittings in (b) are 16, 20, 38, and 39 kHz from top to bottom.

temperature, the same trend is seen: organic mixing yielded a splitting of 16 kHz whereas aqueous mixing yielded a coupling of 31 kHz. Since χ_1 and χ_2 torsional motion is inherently non-uniaxial, the $\bar{\eta} = 0$ line shape (Figure 2a) at high temperatures cannot be solely due to the side chain motion, but the helix backbone must undergo uniaxial rotation faster than the rigid-limit ^{2}H quadrupolar coupling of 125 kHz. Moreover, since the backbone motion should have a higher energy barrier than side chain motion, the couplings of 26−31 kHz in the aqueous sample (Figure 2b) must reflect χ_1/χ_2 torsional motions while the backbone rotation has stopped.

The different backbone mobility of M2TMP in the two sample preparation methods suggests different aggregation states of the protein. Mixing the peptide and lipid in organic solvents before the assembly of lipid bilayers in water may result in a homogeneously mixed membrane mixture in which the tetrameric bundles are well isolated from each other. In contrast, mixing M2TMP with preformed lipid vesicles may not fully solubilize the peptide in the membrane, leading to aggregates of tetramers that inhibit fast rotation on the ^{2}H time scale.

To confirm the backbone motion of the helical bundles in the organic samples, we measured the ^{2}H spectra of d_3-A29 labeled L38F-M2TMP in DLPC and POPC bilayers above and below the T_m of 271 K. Since the Ala methyl group is directly attached to the backbone, there is no side chain torsional motion other than the methyl three-site jump, and quadrupolar couplings smaller than 40 kHz must be attributed to backbone reorientation. Figure 3 shows that above T_m, the peptide exhibits uniaxial lineshapes and 16 kHz couplings in both DLPC and POPC membranes, confirming that the helical bundles undergo fast uniaxial rotation. Below T_m, between 243 and 262 K, the ^{2}H spectra broaden to 32 kHz in the DLPC membrane and 39 kHz in the POPC membrane. The prediction that rotational diffusion should be slower in the thicker membrane (larger h) is confirmed by the larger quadrupolar couplings in the gel-phase POPC membrane at the same reduced temperature as the DLPC sample. In addition, the zero-frequency signal is more completely suppressed in POPC bilayers than in DLPC bilayers.

The fact that the M2TMP spectra in the Lα-phase are the same between DLPC and POPC membranes with different h suggests that as long as the rotational diffusion rate exceeds the coupling strength, it gives the same motionally averaged couplings, which depend only on the orientation of the spin interaction tensor, in this case the Cα-Cβ bond, with respect to the bilayer normal. Equation (1) indicates that an order parameter can be defined: $S \equiv \bar{\delta}/\delta = \bar{\delta}/40$ kHz, that is related to the angle θ of the Cα-Cβ bond relative to the bilayer normal as $S = (1/2)(3\cos^2\theta - 1)$. Thus, the measured splitting of 16 kHz in fluid DLPC and POPC membranes indicates a Cα-Cβ bond orientation of 39° (or 141°) for $S = +0.4$ or 75° (or 105°) for $S = -0.4$. The existing M2TMP tetramer model gives a Cα-Cβ bond orientation of 92°, in reasonable agreement with one of the predicted values (105°). However, this Ala Cα-Cβ constraint, while easy to obtain, is not very sensitive to the helix axis orientation because the Cα-Cβ bond is roughly perpendicular, rather than parallel, to the helical axis. It has been shown that multiple Ala CD_3 groups need to be measured to obtain accurate helix tilt angles.[39]

Rates of M2TMP uniaxial rotational diffusion

We characterized the rotational diffusion rates of the M2TMP tetramers by ^{13}C cross-polarization (CP) MAS spectra as a function of temperature. Figure 4 shows the ^{13}Cα signals of L40 and G34 in DLPC membrane between 258 and 318 K. The sample was prepared by organic-phase mixing. The two Cα signals are strong below the phase transition temperature, disappear between 288 and 298 K, then reappear above 313 K. The same trend is observed in the organic POPC membrane whereas the aqueous POPC sample showed strong signals that are independent of temperature (spectra not shown). The suppression of the ^{13}C signals at intermediate temperatures in the organic samples is a classic signature that motions with similar rates as the C−H dipolar coupling and the ^{1}H decoupling strength, 20,000−50,000 s^{-1}, are present.[40] When this motion is either frozen or sped up by varying the temperature, the ^{13}C signals reappear.

Motions with rates of 10^5 s^{-1} are readily detectable in rotating-frame spin−lattice relaxation time ($T_{1\rho}$) measurements. Figure 5a shows the ^{13}C-detected L40 Hα $T_{1\rho}$ relaxation curves at various temperatures under a ^{1}H spin-lock field of 62.5 kHz. In the aqueous POPC membrane, the peptide has a long ^{1}H $T_{1\rho}$ of >5 ms that is independent of the temperature between 298 and 313 K. In contrast, the organic DLPC sample gave much shorter and temperature-dependent ^{1}H $T_{1\rho}$ values. Above T_m, the ^{1}H $T_{1\rho}$ is only 0.8 ms whereas below T_m, the ^{1}H $T_{1\rho}$ increases to 3.45 ms at 258 K. Figure 5b plots the ^{1}H $T_{1\rho}$ of the lipid CH_2 and L40 Hα in the two samples as a function of temperature. The lipid CH_2 groups show increasing $T_{1\rho}$ with

(39) Strandberg, E.; Wadhwani, P.; Tremouilhac, P.; Durr, U. H.; Ulrich, A. S. *Biophys. J.* **2006**, *90* (5), 1676−1686.
(40) Rothwell, W. P.; Waugh, J. S. *J. Chem. Phys.* **1981**, *74*, 2721−2732.

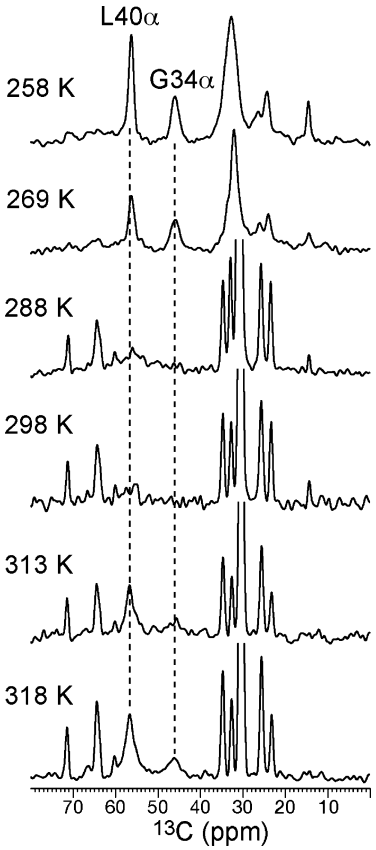

Figure 4. Temperature-dependent ^{13}C spectra of [^{13}Cα-L40,^{13}Cα-G34] M2TMP in DLPC membrane prepared by organic mixing. Below T_m (271 K), the L40α and G34α signals are strong. With increasing temperature, the peak intensities decrease and almost disappear due to intermediate time scale motion (288−298 K). The signals reappear as the peptide reaches the fast motion limit (313−318 K).

increasing temperature, indicating that they are in the fast motional limit in the temperature range examined (Figure 5c). The organic DLPC sample shows decreasing $T_{1\rho}$ with increasing temperature, indicating that the peptide motion is near the minimum of the $T_{1\rho}$ curve. Finally, the temperature-independence and long $T_{1\rho}$ of the aqueous POPC sample indicates that M2TMP is in the slow motional limit.

Amplitudes of backbone motion from ^{13}C-^{1}H dipolar coupling and ^{13}C CSA

Direct evidence of backbone motion can be obtained from Cα-Hα dipolar couplings and Cα CSAs. Figure 6 shows the L40 Cα-Hα dipolar coupling curves in three different samples obtained from the indirect dimension of the 2D DIPSHIFT spectra. In the aqueous POPC membrane, a coupling of 10.6 kHz was measured (Figure 6a). Taking into account the MREV-8 scaling factor (0.47), this corresponds to an unscaled coupling of 22.6 kHz, which is the rigid limit C−H dipolar coupling. In contrast, POPC and DLPC organic membranes (b, c) gave significantly reduced couplings of 3.4 kHz and 4.0 kHz, respectively, which correspond to order parameters of ± 0.32 and ± 0.37. The sign degeneracy, similar to the ^{2}H quadrupolar interaction, is due to the uniaxial nature of the dipolar interaction. The negative S values indicate a Cα-Hα angle of 70° (110°) for POPC and 73° (107°) for DLPC with respect to the bilayer normal. The existing M2TMP structural model, obtained from experiments conducted on DMPC bilayers, gives a Cα-Hα orientation of 73° or 107° from the bilayer normal, in

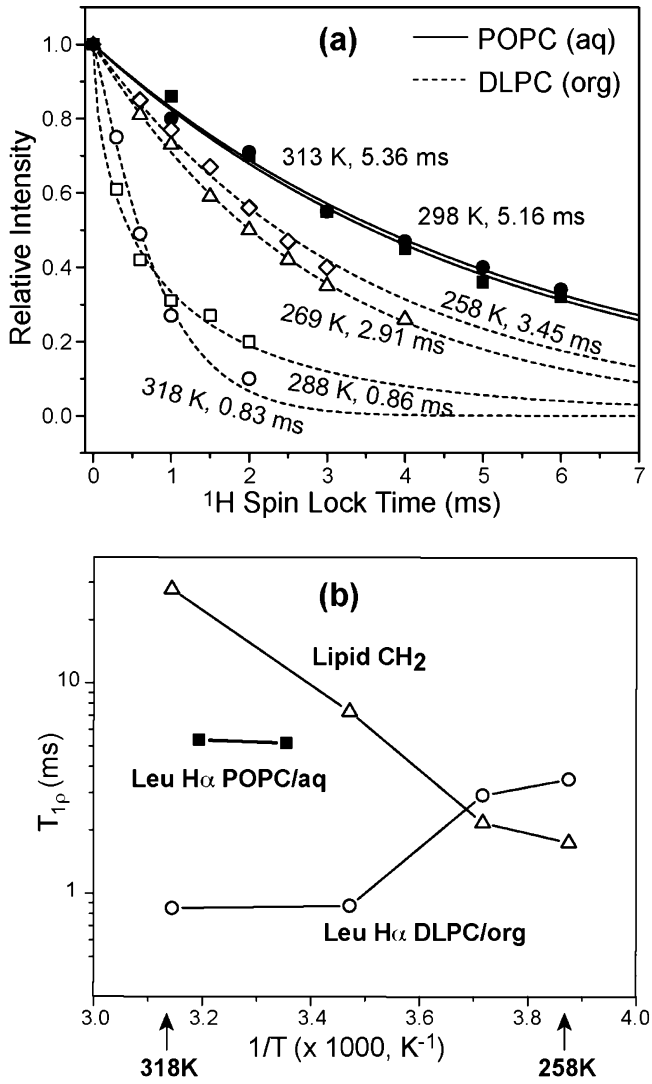

Figure 5. Temperature-dependent ^{1}H $T_{1\rho}$ of M2TMP in different lipid membranes. (a) ^{13}C-detected ^{1}H $T_{1\rho}$ curves of L40α at various temperatures. The aqueous POPC sample is shown with filled symbols and solid fit curves. The organic DLPC sample is shown with open symbols and dashed fit curves. (b) ^{1}H $T_{1\rho}$ versus inverse temperature for lipid CH_2 and L40α in the organic DLPC sample, and L40α in the aqueous POPC sample.

excellent agreement with the present data. The similarity of the two C−H couplings belies the fact that the helix orientation is detectably different between the two membranes, as we show by ^{15}N experiments below. Again, this is a result of the roughly perpendicular orientation of the Cα-Hα bond to the helix axis, which makes it less sensitive than the N−H dipolar coupling to the helix tilt angle.

The same backbone uniaxial rotation also averages the Cα CSA, which can be measured under MAS using the recoupling experiment SUPER.[33,41] Figure 7 shows the CSA spectra of L40 in various membranes, obtained from the indirect dimension of the 2D SUPER spectra. Only the organic DLPC sample in the liquid crystalline phase shows a motionally narrowed CSA ($\bar{\delta}$=9.2 ppm) while the gel-phase sample or aqueous samples gave CSAs of 18 ppm, which is the rigid-limit CSA of α-helical Leu predicted by quantum chemical calculations.[42]

(41) Tycko, R.; Dabbagh, G.; Mirau, P. A. *J. Magn. Reson.* **1989**, *85*, 265−274.
(42) Sun, H.; Sanders, L. K.; Oldfield, E. *J. Am. Chem. Soc.* **2002**, *124*, 5486−5495.

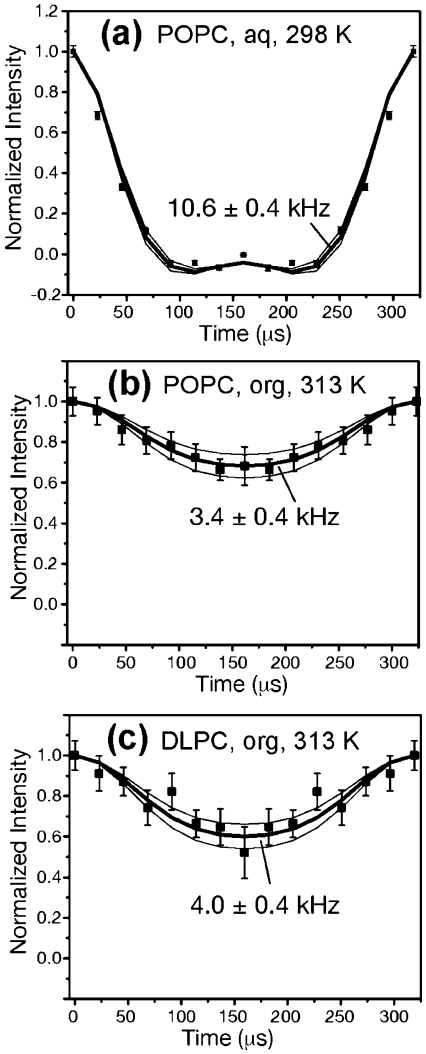

Figure 6. $^{13}C-^{1}H$ DIPSHIFT curves of $^{13}C\alpha$-L40 in M2TMP in different membrane samples. (a) POPC aqueous sample (P/L = 1:20). (b) POPC organic sample (P/L = 1:15). (c) DLPC organic sample (P/L = 1:15). The POPC aqueous sample (a) gave a rigid-limit $^{13}C-^{1}H$ dipolar coupling, whereas the two organic samples (b, c) have motionally averaged dipolar couplings.

M2TMP orientation from powder samples using ^{15}N NMR

To determine the orientation of α-helical peptides with high angular resolution, the most sensitive nuclear spin interactions are the N−H dipolar coupling and ^{15}N CSA, as both tensors are roughly parallel to the helix axis. The PISEMA experiment, commonly used for aligned samples, correlates these two spin interactions in a 2D spectrum, producing wheel-like patterns called "PISA wheels". The size and frequency position of the PISA wheels depend on the tilt angle of the helices whereas the residue position on the wheel depends on the rotation angle around the helix axis.[43,44] Figure 8a shows the calculated PISA wheels for tilt angles of 15°−45° for 0°-aligned membranes. The center of the wheels shifts toward lower frequencies in both dimensions as the tilt angle increases. When the alignment axis is perpendicular to the magnetic field, and the protein undergoes fast rotational diffusion, "90° PISA wheels" are obtained that are half-sized mirror images of the 0° PISA wheels (eq 2),

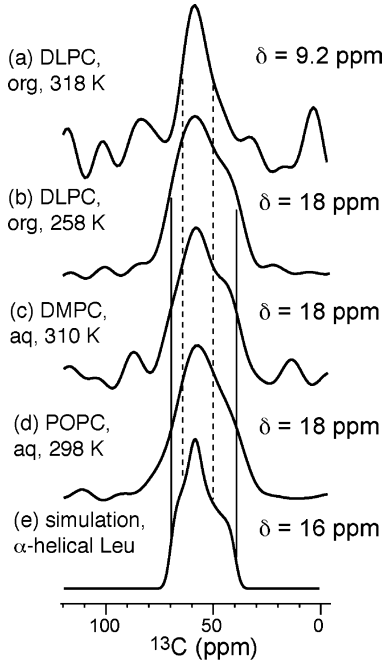

Figure 7. ^{13}C CSA spectra of the $^{13}C\alpha$-L40 in M2TMP in various membranes, extracted from the indirect dimension of 2D SUPER spectra. (a) DLPC organic sample at 318 K. (b) DLPC organic sample at 258 K. (c) DMPC aqueous sample at 310 K. (d) POPC aqueous sample at 298 K. Spectra (b−d) show rigid-limit CSAs, as simulated in (e). Spectrum (a) is the only one narrowed by fast backbone motion of the peptide.

reflected around the isotropic shift and zero dipolar coupling axis (Figure 8b). These 90° wheels have been observed in membrane proteins bound to "unflipped" bicelles.[45]

The presence of protein uniaxial rotation enables PISA wheels to be obtained from powder samples using MAS and static experiments. For example, N−H dipolar couplings can be measured in a site-specific fashion using the 2D DIPSHIFT[46] or LG-CP[47] experiments under MAS, giving the $\bar{\delta}_{//}$ frequency or 0° dipolar coupling. The ^{15}N CSA can be obtained from the $\bar{\delta}_{\perp}$ singularity of the static ^{15}N spectra of site-specifically labeled samples or by CSA recoupling experiments under MAS on multiply labeled samples. When the 0° dipolar coupling is correlated with the 90° chemical shift, we obtain 0°/90° PISA wheels (Figure 8c). Whichever PISA wheels are used, multiple ^{15}N-labeled residues are necessary to determine both the tilt and the rotation angles of the helix.

We demonstrate this powder orientation determination approach by measuring the ^{15}N chemical shift and N−H dipolar couplings of site-specifically labeled M2TMP. Figure 9 shows static ^{15}N spectra of M2TMP in DLPC and POPC organic membranes. L26, V28, and A30 were ^{15}N-labeled to cover different rotational angles around the helix axis. Most spectra show well-defined $\bar{\delta}_{\perp}$ singularities, $\bar{\delta}_{//}$ edges, and $\bar{\eta} = 0$ lineshapes and a "magic-angle hole" at the isotropic shift. This magic-angle hole results from the collinearity of the chemical shift tensor and the dipolar coupling tensor in uniaxially mobile molecules.[48] The exception is V28, whose $\bar{\delta}_{\perp}$ singularity nearly

(43) Marassi, F. M.; Opella, S. J. *J. Magn. Reson.* **2000**, *144*, 150−155.
(44) Wang, J.; Denny, J.; Tian, C.; Kim, S.; Mo, Y.; Kovacs, F.; Song, Z.; Nishimura, K.; Gan, Z.; Fu, R.; Quine, J. R.; Cross, T. A. *J. Magn. Reson.* **2000**, *144*, 162−167.
(45) Park, S. H.; Mrse, A. A.; Nevzorov, A. A.; De Angelis, A. A.; Opella, S. J. *J. Magn. Reson.* **2006**, *178*, 162−165.
(46) Munowitz, M.; Aue, W. P.; Griffin, R. G. *J. Chem. Phys.* **1982**, *77*, 1686−1689.
(47) vanRossum, B. J.; deGroot, C. P.; Ladizhansky, V.; Vega, S.; deGroot, H. J. M. *J. Am. Chem. Soc.* **2000**, *122*, 3465−3472.
(48) Yamaguchi, S.; Huster, D.; Waring, A.; Lehrer, R. I.; Tack, B. F.; Kearney, W.; Hong, M. *Biophys. J.* **2001**, *81*, 2203−2214.

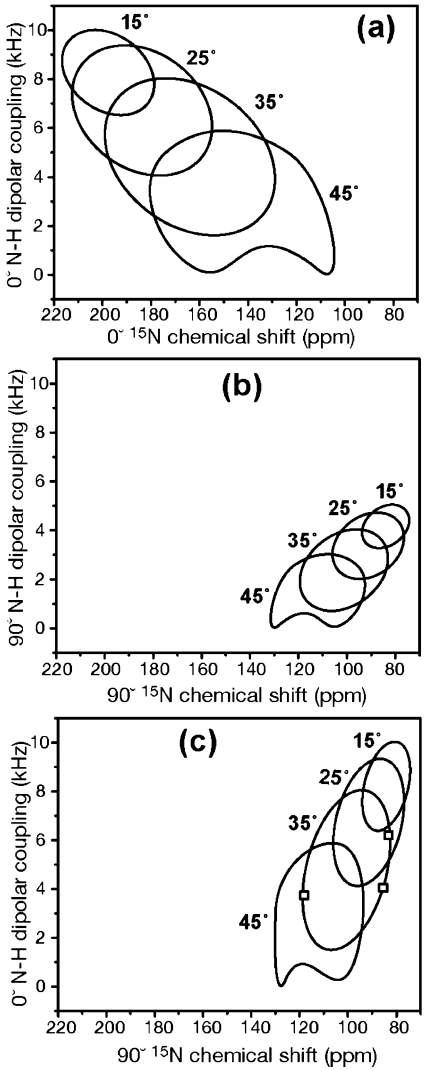

Figure 8. Calculated PISA wheel spectra for (a) 0°-aligned membranes, (b) 90°-aligned membranes, and (c) 0° N−H coupling and 90° ^{15}N chemical shift from unoriented membranes. Tilt angles of 15°−45° are shown. In (c), the resonances of A30, V28, and L26 at a tilt angle of 35° and with rotation angles reproducing the previous glass-plate aligned data are shown.[11]

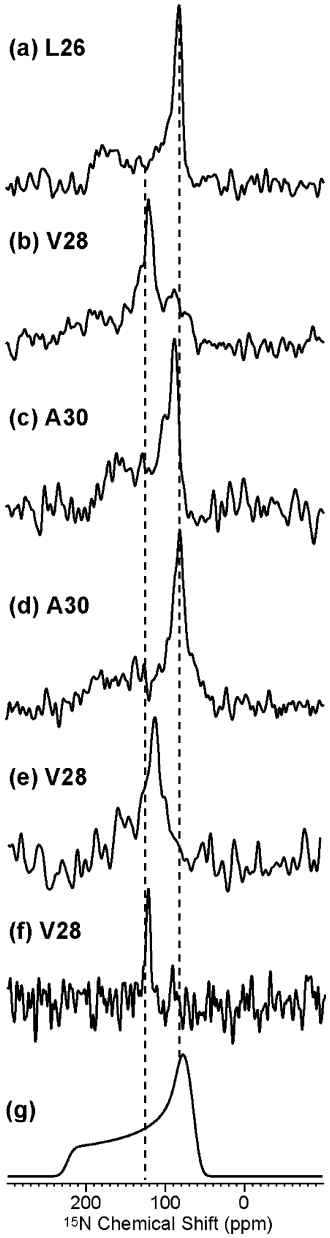

Figure 9. ^{15}N static spectra of ^{15}N-labeled M2 peptides in DLPC and POPC bilayers. (a) L26 of M2TMP in DLPC bilayers. (b) V28 of M2TMP in DLPC bilayers. (c) A30 of M2TMP in DLPC bilayers. (d) A30 of L38F-M2TMP in POPC bilayers. (e) V28 of M2TMP in POPC bilayers. (f) V28 of M2(19−60) in DLPC bilayers. (g) Calculated rigid-limit ^{15}N powder pattern.

coincides with the isotropic shift in various samples so that the magic-angle hole is not visible (Figure 9b, e, f). This indicates that the V28 main ^{15}N chemical shift tensor axis, which is near its N−H bond, is incidentally aligned near the magic angle with respect to the bilayer normal, so that the CSA tensor is motionally averaged to vanishing anisotropies. Also observed is a 6 ppm difference in the A30 $\bar{\delta}_\perp$ frequency between DLPC and POPC bilayers (Figure 9c, d), indicating that the helix orientation differs between the two lipid bilayers.

Figure 10 shows the N−H dipolar-doubled DIPSHIFT curves of the same ^{15}N labeled residues. A range of couplings from 2.6 kHz to 8.5 kHz is observed. After taking into account the dipolar doubling and MREV-8 scaling factor, we find unscaled couplings from 4.7 kHz to 9.0 kHz (Table 1). The rigid-limit one-bond N−H dipolar coupling is 10.5 kHz, thus these N−H bonds are variably tilted from the bilayer normal.

Figure 11 summarizes the N−H dipolar coupling and the $\bar{\delta}_\perp$ ^{15}N chemical shift of A30, V28, and L26 in DLPC and POPC bilayers. Superimposed on the experimental data are the best-fit 0°/90° PISA wheels calculated using the ideal α-helical geometry. The DLPC data (filled squares) are best fit to a 0°/90° PISA wheel of $\tau = 35° \pm 3°$. The rotation angle, determined by the relative positions of the three sites on the wheel, is 105°, where $\rho = 0°$ is defined by the Ser_{22} CO−Ser_{23} N peptide bond direction. With the same reference, the oriented-membrane ^{15}N data gave a rotation angle of ∼95°.[11] L26 shows an ^{15}N chemical shift that falls outside the calculated 35° PISA wheel, but the measured N−H dipolar coupling is consistent with the predicted frequency for $\tau = 35°$. This may result from a deviation of the ^{15}N chemical shift tensor magnitude or orientation at this site from the literature value used in the simulation of the PISA wheel. Indeed, ^{15}N chemical shift tensor variations in proteins can be significant, as shown by a recent study of the protein

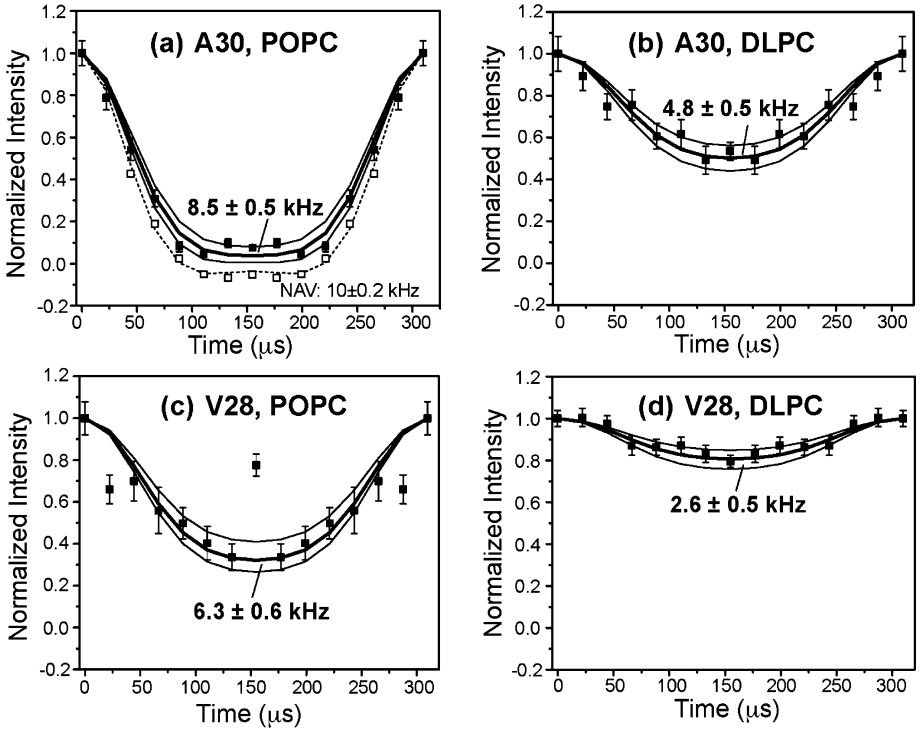

Figure 10. N−H dipolar-doubled DIPSHIFT curves of selected residues of M2TMP in DLPC and POPC bilayers. (a) A30 of L38F−M2TMP in POPC bilayers. (b) A30 of M2TMP in DLPC bilayers. (c) V28 of M2TMP in POPC bilayers. (d) V28 of M2TMP in DLPC bilayers. The DIPSHIFT curve of crystalline rigid *N*-acetyl-valine (NAV) is shown in (a) for comparison. The best-fit N−H dipolar coupling (bold solid lines) is indicated for each site. All spectra were measured at 313 K under 3.23 kHz MAS.

Table 1. ^{15}N 90° Chemical Shifts (ω_N) and N−H Dipolar Couplings (ω_{NH}) of Several Residues in M2 Peptides in Various Lipid Membranes

^{15}N-labeled peptide	lipid bilayer	ω_N (ppm)	ω_{NH} (kHz)
L26, M2TMP	DLPC	78 ± 3	4.8
V28, M2TMP	DLPC	117 ± 4	2.8
V28, M2TMP	POPC	106 ± 4	6.3
V28, M2(19−60)	DLPC	123 ± 3	NA
A30, M2TMP	DLPC	87 ± 2	5.1
A30, L38F-M2TMP	POPC	81 ± 3	9.0

GB1.[49] Fortunately, the dipolar coupling information is intrinsically more accurate, which is the reason that N−H dipolar couplings only are used in the dipolar wave analysis for orientation determination.[50] In POPC bilayers, the A30 and V28 data are best fit by a tilt angle of 26° ± 3° and the same rotation angles. The N−H dipolar couplings are significantly larger than those in DLPC bilayers, and the $\bar{\delta}_\perp$ chemical shifts are further away from the isotropic chemical shift. Both indicate larger anisotropies, which shift the 0°/90° PISA wheels to a smaller tilt angle. Interestingly, as the PISA wheels become smaller, the tilt angle resolution improves; thus, although the rotation angle is defined only by two residues, the precision of the tilt angle is still high.

The comparison between the DLPC and POPC data indicates clearly that the M2TMP helix tilt angle is affected by the membrane thickness: increasing the membrane thickness decreases the tilt angle, as expected for the hydrophobic thickness of the peptide to match the hydrophobic thickness of the lipid bilayer. The similar rotation angle between the two membranes

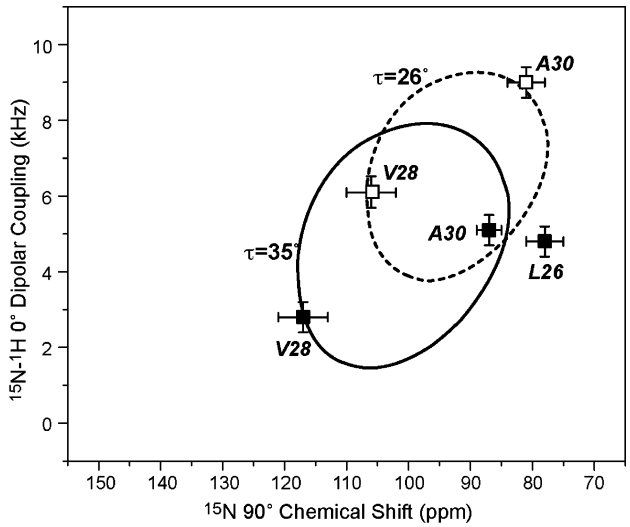

Figure 11. Orientation of M2TMP using 0°/90° PISA wheels constructed from data collected from unoriented samples. The DLPC membrane results of A30, V28, and L26 are shown in filled squares and solid lines. The POPC membrane data are shown in open squares and dashed lines.

is also expected, since the residues facing the pore lumen must be maintained to carry out the proton-conducting function.[51] Mutation of key channel-facing residues can destabilize the channel.[10,52]

The tilt angle of 35 ± 3° in the DLPC membrane is similar to, instead of larger than, the tilt angle found in the thicker DMPC membrane.[11] This may be a result of the competition

(49) Wylie, B. J.; Franks, W. T.; Rienstra, C. M. *J. Phys. Chem. B* **2006**, *110*, 10926−10936.
(50) Mesleh, M. F.; Lee, S.; Veglia, G.; Thiriot, D. S.; Marassi, F. M.; Opella, S. J. *J. Am. Chem. Soc.* **2003**, *125*, 8928−8935.
(51) Pinto, L. H.; Dieckmann, G. R.; Gandhi, C. S.; Papworth, C. G.; Braman, J.; Shaughnessy, M. A.; Lear, J. D.; Lamb, R. A.; DeGrado, W. F. *Proc. Natl. Acad. Sci. U.S.A.* **1997**, *94*, 11301−11306.
(52) Wang, C.; Lamb, R. A.; Pinto, L. H. *Biophys. J.* **1995**, *69*, 1363−1371.

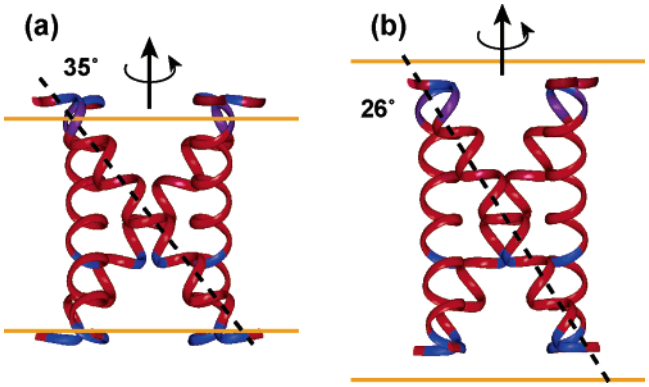

Figure 12. Orientation of M2TMP helical bundles in membranes of different thicknesses. (a) DLPC bilayer. (b) POPC bilayer. The P−P boundaries of the bilayer are shown in orange. The peptide lengths and P−P distances are shown to scale. Red: hydrophobic residues. Blue: polar and charged residues. The tilt angle of M2TMP is 35° in DLPC bilayers and 26° in POPC bilayers.

between increasing the tilt angle to minimize the hydrophobic mismatch and the need to maintain channel stability through sufficient hydrophobic contacts between the residues on different helices. The similarity suggests that a tilt angle of 35°−38° is the maximum achievable for this peptide while still maintaining its tetrameric state.

Below this maximum tilt angle, M2TMP orientation appears to still depend on the membrane thickness. The current result that the peptide orientation differs between DLPC and POPC bilayers supports a recent EPR study showing that the intermolecular distance between spin-labeled M2 helices changes with the membrane thickness.[20] The previous observation by Cross and co-workers that the M2TMP orientation does not change significantly between DMPC and DOPC bilayers[19] may be coincidental: DOPC lipids differ from DMPC lipids not only in the chain length but also in having a double bond in each chain, thus the lateral pressure of the two membranes differs. The unsaturated DOPC bilayer may laterally expand to adopt a similar thickness as the saturated DMPC bilayer, thus giving the same tilt angle for the M2 helices.

Figure 12 summarizes the orientation of M2TMP determined from the current study. M2TMP shows different tilt angles between DLPC and POPC bilayers. The P−P distances of the two membranes are ∼30 Å and ∼45 Å, respectively. The 25-residue M2TMP has a length of 37.5 Å if the ideal rise of 1.5 Å per residue is used. Thus a tilt angle of 35° and 26° yields, respectively, a vertical length of 31 Å and 34 Å, respectively. The former agrees well with the DLPC P−P distance, while the latter is shorter than the POPC P−P distance but closer to the average between the estimated POPC hydrophobic thickness of 27 Å and the P−P distance.[20]

M2(19−60) Orientation from Powder Samples Using ^{15}N NMR. Finally, we apply this powder orientation determination technique to a longer construct of the M2 protein, M2(19−60), whose orientation has not been determined before. This construct encompasses all the structured regions of the M2 protein and has been shown to be functional in oocytes.[7] With a molecular weight of 4878, the M2(19−60) peptide would be more difficult to align than M2TMP. Figure 9e shows the static ^{15}N spectrum of V28 in M2(19−60) bound to DLPC bilayers; a chemical shift of 123 ppm is observed, similar to the value found for M2TMP in the same membrane. Since the rotation angle of the protein is fixed, the similarity in the ^{15}N CSA indicates that M2(19−60) has the same tilt angle as M2TMP within experimental uncertainty. This implies that structural conclusions made on the M2TMP helical bundle can be reasonably extrapolated to the longer peptide. Interestingly, the V28 ^{15}N line shape in M2(19−60) is much narrower than in M2TMP, suggesting that the inclusion of the extra membrane residues creates a conformationally more homogeneous peptide.

Although a complete investigation of M2(19−60) is beyond the scope of the current paper, the data is quite interesting with respect to the role of the C-terminal helix in influencing the properties of the M2 proton channel. Previous studies of M2TMP suggested that the tetramer formed by this peptide had multiple conformations, some of which could be stabilized by specific mutations to its sequence.[53] The decrease in heterogeneity in M2(19−60) versus M2TMP suggests that the C-terminal helix helps stabilize one or a small subset of conformations within the transmembrane helix. Furthermore, the C-terminal helix lies just C-terminal to, and structurally interacts with, the His_{37}-Trp_{41} pair that forms the proton selectivity filter in M2. Thus, it might modulate the properties of this essential motif, which is known to be required for proton conduction. Finally, while we have not yet made measurements involving labeled residues in the C-terminal helix, it is clear that the present approach has considerable promise for examining the conformation of this region of the protein.

Conclusion

We have shown that, in the presence of fast uniaxial rotational diffusion, orientation-dependent PISA wheels in a 2D N−H/N correlation pattern can be obtained from unoriented membrane protein samples. This allows membrane protein orientation to be determined without macroscopic alignment, thus offering an important opportunity for studying membrane proteins that naturally disrupt lipid bilayers or that are difficult to align. In this work the M2TMP samples are studied under conditions where the peptide forms tetrameric helical bundles, as determined by separate ^{19}F spin diffusion experiments. Thus, the observed fast uniaxial motion of the whole helical bundle, with a total molecular weight of 10.9 kDa, indicates that membrane proteins with an effective size smaller than 100 residues have the requisite uniaxial mobility to give orientation-dependent NMR spectra for interactions as large as the ^{2}H quadrupolar coupling. However, since the spin interactions most sensitive to helix orientations are ^{15}N-related tensors, the minimum required rotational diffusion rate is much lower (Figure 1), and membrane proteins with a radius as large as 30 Å should be accessible to this powder sample approach using ^{15}N NMR. Further experiments are necessary to show whether fast uniaxial rotations compared to the ^{15}N NMR time scale are indeed general in larger proteins. In addition to the protein molecular weight, the P/L ratio may also affect the uniaxial rotational rate. The motionally averaged spectra shown here were obtained from samples containing relatively high mass concentrations of peptide, ∼20%. This suggests that it is not necessary to lower the protein concentration significantly to ensure motion. Instead, it is more important to maintain the protein or peptide assembly in their natural functional states without nonspecific aggregation,

(53) Stouffer, A. L.; Nanda, V.; Lear, J. D.; DeGrado, W. F. *J. Mol. Biol.* **2005**, *347*, 169−179.

as indicated by the dramatically different mobilities observed between the organically mixed and aqueous mixed M2TMP samples.

The powder samples allow MAS experiments to be used for orientation determination. Combining ^{13}C and ^{15}N labeling, one can in principle employ multidimensional correlation experiments to simultaneously extract multiple orientational constraints. While for demonstration we only measured site-specifically ^{15}N-labeled samples here, the 2D N−H DIPSHIFT and ^{15}N CSA filter experiments can be extended to three dimensions, where an additional ^{13}C chemical shift dimension can be used to resolve multiple residues in the protein. The main challenge will be to conduct these experiments in the liquid-crystalline phase of the membrane where the protein is mobile, with motionally averaged dipolar couplings for polarization transfer.

Acknowledgment. We thank Tim Doherty for help with the synthesis of Fmoc-protected amino acids. This work is supported by NSF Grant MCB-0543473 to M.H. and NIH Grant GM56423 to W.F.D.

JA070305E